Structural and Dielectric Properties of $Bi_3Ti_{1.5}W_{0.5}O_9$

© S.V. Zubkov [1], I.A. Parinov [2], Yu.A. Kuprin [1], A.V. Nazarenko [3]

[1] Scientific Research Institute of Physics, Southern Federal University,
Rostov-on-Don, Russia
[2] Vorovich Institute of Mathematics, Mechanics and Informatics, Southern Federal University,
Rostov-on-Don, Russia
[3] Southern Scientific Center, Russian Academy of Sciences,
Rostov-on-Don, Russia

E-mail: svzubkov61@mail.ru

Layered perovskite-like oxide $Bi_3Ti_{1.5}W_{0.5}O_9$ has been synthesized by the method of high-temperature solid-state reaction. The X-ray diffraction study showed that the compound is single-phase and has the structure of the family of Aurivillius phases (AP) with parameters close to the orthorhombic unit cell corresponding to the space group $A2_1am$. The temperature dependences of the relative permittivity $\varepsilon/\varepsilon_0$ and the loss tangent $\mathrm{tg}\,\sigma$ are measured at different frequencies. For the synthesized compound, the piezoelectric modulus d_{33} was measured. The microstructure of $Bi_3Ti_{1.5}W_{0.5}O_9$ has been obtained.

Keywords: Aurivillius phases, $Bi_3Ti_{1.5}W_{0.5}O_9$, activation energy E_a, Curie temperature T_C, piezoelectric modulus d_{33}.

1. Introduction

In 1949, when studying the system $Bi_2O_3-TiO_2$, V. Aurivillius established formation of the oxide $Bi_4Ti_3O_{12}$ with the perovskite-type structure [1]. Then, during two years he had produced several oxides with the similar structure [2,3]. However, at the first stage Aurivillius limited himself by studying a structure of the produced compounds only. Only ten years later, Smolensky, Isupov and Agranovskaya [4] had discovered ferroelectric properties of Bi_2PbNbO_9, which belongs to this class of compounds. Several dozens of Aurivillius phases were produced subsequently and almost all of them turned out to be ferroelectrics [5–10]. The Aurivillius phases (AP) form a large family of bismuth-containing lamellar compounds of the perovskite type, whose chemical composition is described by the general formula $A_{m-1}Bi_2B_mO_{3m+3}$. The crystal structure of the AP family consists in alternating layers $[Bi_2O_2]^{2+}$, separated by m perovskite-like layers $[A_{m-1}B_mO_{3m+1}]^{2-}$, where A — long-radius ions (Bi^{3+}, Ca^{2+}, Gd^{3+}, Sr^{2+}, Ba^{2+}, Pb^{2+}, Na^+, K^+, Y^{3+}, Ln^{3+} (lanthanides)) have dodecahedral coordination, and B — positions within oxygen octahedrons are occupied with heavily charged ($\geq 3+$) short-radius cations (Ti^{4+}, Nb^{5+}, Ta^{5+}, W^{6+}, Mo^{6+}, Fe^{3+}, Mn^{4+}, Cr^{3+}, Ga^{3+}, etc.). The value m is determined by a number of perovskite layers $[A_{m-1}B_mO_{3m+1}]^{2-}$, located between fluorite-like layers $[Bi_2O_2]^{2+}$, and may take an integer number or a half-integer within the range $1-5$ (Fig. 1). If m — a half-integer, then the lattice has alternative perovskite layers with m, differing by 1. For example, at $m = 1.5$ the lattice has an equal number of the layers with $m = 1$

and $m = 2$. For example, the value $m = 1$ corresponds to the compound Bi_2WO_6, $m = 2$ corresponds to Bi_2PbNbO_9, $m = 3$ corresponds to $Bi_4Ti_3O_{12}$, $m = 4$ corresponds to $Bi_4CaTi_4O_{15}$, $m = 5$ corresponds to $Bi_4Sr_2Ti_5O_{18}$. The positions A and B may be occupied with the same atom or several different atoms. Atomic replacements in the positions A and B substantially affect electrophysical AP characteristics. In particular, there are big changes of the values of permittivity, conductivity, and, besides, the Curie temperature T_C can also change in a wide range. Thus, study of the cation-replaced AP compounds can play an important role in creating materials for various technological applications. The structure of the AP compounds $Bi_2A_{m-1}B_mO_{3m+3}$ above the Curie point T_C is tetragonal and belongs to the spatial group $I4/mmm$. The type of the spatial group below the Curie point T_C depends on a value of the number m. For the odd m of the spatial group of the ferroelectric phase it is $B2cb$ or $Pca2_1$, for the even m it is $A2_1am$, and for the half-integer m it is $Cmm2$ or $I2cm$.

Scientific interest in synthesis and study of new AP compounds is stimulated by numerous examples of their use in various electronic devices, due to their unique physical properties (piezoelectric, ferroelectric, etc.). They exhibit low temperature coefficients of dielectric and piezoelectric losses, as well as low aging temperatures in addition to high Curie temperatures ($T_C \leq 965°C$) [11,12].

For the first time, in 1976 Kikuchi synthesized $Bi_3Ti_{1.5}W_{0.5}O_9$ [13], and in 2005 Hyatt published his study of the crystal structure $Bi_3Ti_{1.5}W_{0.5}O_9$ [14]. The purpose of this study was to investigate a micro- and crystal-structure, piezo- and dielectric-characteristics of the

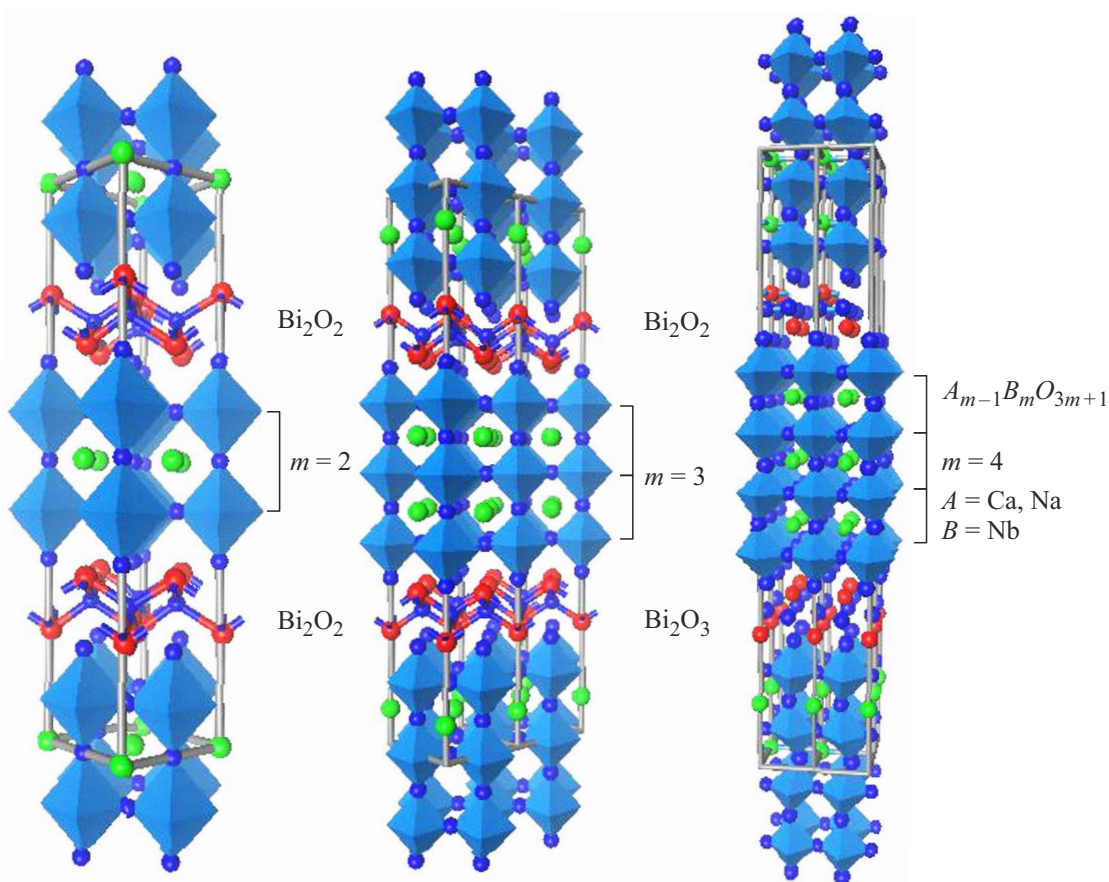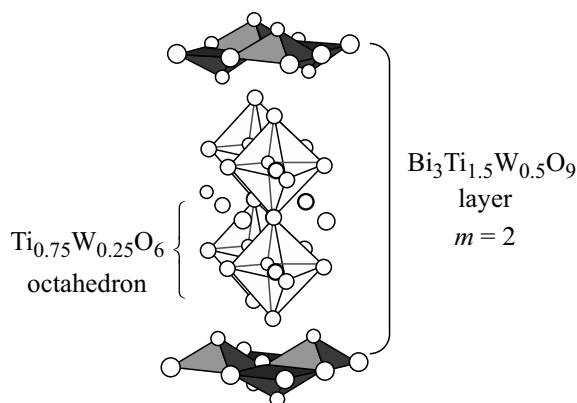**Figure 1.** AP structures with $m = 2, \ 3, \ 4$.

Figure 2. Structures $Bi_3Ti_{1.5}W_{0.5}O_9$ with $m = 2$.

compound $Bi_3Ti_{1.5}W_{0.5}O_9$ (see Fig. 2) and to measure a phase transition temperature.

2. Experiment

A polycrystalline AP sample was synthesized via the solid-state reaction of respective oxides Bi_2O_3, TiO_2, WO_3, all the initial compounds were of a pure-for-analysis grade. After weighing in a stoichiometric composition and thorough fining of the initial oxides with addition of ethanol, the pressed samples were ignited at the temperature of $770°C$ during 4 h. The samples were calcinated in a muffle furnace in air. The sample was then crushed, repeatedly fined and pressed into pills of a diameter 10 and a thickness of 1.0×1.5 mm, with subsequent final AP synthesis at the temperature of $1100°C$ (2 h). The X-ray image was recorded at a diffractometer Rigaku Ultima IV with a Cu-X-ray tube. Radiation Cu$K\alpha 1$, $\alpha 2$ was picked up out of the general spectrum by means of a Ni-filter. The X-ray image was measured within an angle range 2θ from 10 to $60°$ with a scanning step of $0.02°$ and exposure (intensity recording time) of 4 s per dot. Analysis of the X-ray image profile, determination of line positions, their indexing (hkl) and the refinement of lattice cell parameters was carried out using the software PCW 2.4 [15]. In order to measure the permittivity and electric conductivity, electrodes as discs of a diameter of 10 and thickness of about 1.5 mm were applied onto flat surfaces of the AP samples using Ag-paste annealed at the temperature of $700°C$ (for 1 h). The temperature and frequency dependences of the dielectric characteristics were measured

Table 1. Lattice cell parameters. a_0, b_0, c_0, V, a_t — a parameter of the tetragonal period, c' — an octahedron height along the axis c, $\delta c'$ — non-cubicity, δb_0 — rhombic distortion.

Compound	a_0, Å	b_0, Å	c_0, Å	V, Å^3	c', Å	a_t, %	$\delta c'$, %	δb_0, %
Bi$_3$Ti$_{1.5}$W$_{0.5}$O$_9$	5.3861	5.3742	24.8572	719.51	3.7586	3.8043	-1.2	-0.2

Table 2. Dielectric characteristics of Bi$_3$Ti$_{1.5}$W$_{0.5}$O$_9$: Curie temperature T_C, piezomodule d_{33}, tolerance factor t, relative permittivity $\varepsilon/\varepsilon_0$, activation energy E_n

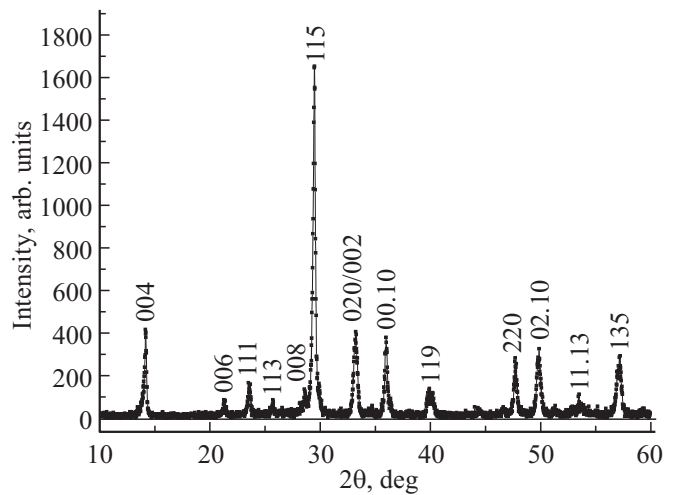| Compound	T_C, °C	d_{33}, pC/N	t	$\varepsilon/\varepsilon_0(T)$ (at 100 kHz)	$E_1/E_2/E_3$, eV
Bi$_3$Ti$_{1.5}$W$_{0.5}$O$_9$	760	8	0.9778	1000	0.67/0.29/0.06

by means of an LCR meter E7-20 within the frequency range from 100 kHz to 1 MHz and within the temperature range from the room temperature to 900°C. The sample was polarized in an oil bath at 125°C at the voltage of 35 kV/cm during 30 min. Cleaved end faces of the sample surface of Bi$_3$Ti$_{1.5}$W$_{0.5}$O$_9$ were imaged in Common Use Center SSC RAS on a 3D-scanning laser microscope KeyenceVK-9700 (Japan), having a short-wave laser (408 nm). The pictures were obtained a reflected light mode by a confocal method, thereby resulting in definition evenly across all the regions under study. The scanning step along the height (axis Z) was 0.08 μm in a Real PeakDetection mode.

3. Results and discussion

The diffraction pattern of a solid solution under study Bi$_3$Ti$_{1.5}$W$_{0.5}$O$_9$ corresponds to a single-phase AP with $m = 2$ and contains no additional isostructural reflection. It was found that the synthesized compound Bi$_3$Ti$_{1.5}$W$_{0.5}$O$_9$ of the AP family crystallizes to an orthorhombic system with the spatial group of the lattice cell $A2_1am$ (No 36). The Fig. 3 shows an experimental powder X-ray image of the compound under study Bi$_3$Ti$_{1.5}$W$_{0.5}$O$_9$.

Parameters and a volume of the lattice cell are determined as per the X-ray diffraction data (Table 1).

The Table 1 also includes parameters of the orthorhombic δb_0 and tetragonal $\delta c'$ deformation; the average tetragonal period a_t, the tolerance factor t and the average thickness of one perovskite layer c'; $c' = 3c_0/(8 + 6m)$ — the thickness of a single perovskite-like layer, $a_t = (a_0 - b_0)/2$ — the average value of the tetragonal period; a_0, b_0, c_0 — the lattice periods; $\delta c' = (c' - a_t)/a_t$ — lattice cell's non-cubicity, i.e. elongation or contraction of the cubic form; $\delta b_0 = (b_0 - a_0)/a_0$ — the rhombic deformation [16–18]. The obtained parameters of the lattice cell of the studied AP samples Bi$_3$Ti$_{1.5}$W$_{0.5}$O$_9$ are close to those determined earlier: $a = 5.4018\,(2)$ Å, $b = 5.3727\,(4)$ Å, $c = 24.9388\,(1)$ Å [14]. The tolerance factor t was introduced by Goldschmidt [19] as a geometric criterion

Figure 3. X-ray image experimental curve of the compound Bi$_3$Ti$_{1.5}$W$_{0.5}$O$_9$.

determining a stability and distortion degree of the crystal structure:

$$t = (R_A + R_O)/[\sqrt{2}(R_B + R_O)], \qquad (2)$$

where R_A and R_B — cation radii in the points A and B, respectively; R_O — an oxygen's ion radius. The present paper calculated the tolerance factor t taking into account the ionic radii as per Shannon [20] for corresponding coordination numbers (CN) (O^{2-} (CN = 6) $R_O = 1.40$ Å, W^{6+} (CN = 6) $R_{W^{6+}} = 0.6$ Å, Ti^{4+} (CN = 6) $R_{Ti^{4+}} = 0.605$ Å).

In order to obtain a distortion degree of an ideal perovskite structure, we have determined the tolerance factor t, which is given in Table 2.

The Shannon table contains no ionic radius Bi^{3+} for coordination with CN = 12. That is why its value was determined based of the ionic radius with CN = 8 ($R_{Bi^{3+}} = 1.17$ Å), multiplied to an approximation factor of 1.179, and for Bi^{3+} (CN = 12) we have obtained $R_{Bi^{3+}} = 1.38$ Å. The results of the structure studies have been supplemented by temperature dependences of relative
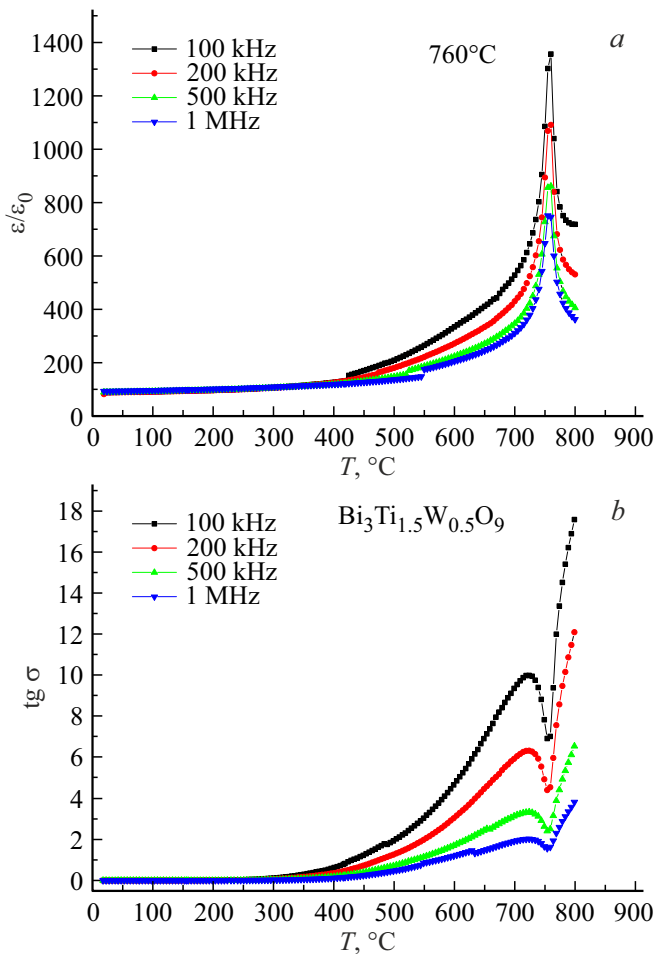
Figure 4. Temperature dependences of the relative permittivity $\varepsilon/\varepsilon_0$ (*a*) and the dielectric loss tangent ($\text{tg}\,\sigma$) (*b*) for $Bi_3Ti_{1.5}W_{0.5}O_9$ at the frequencies from 100 kHz to 1 MHz.

permittivity $\varepsilon/\varepsilon_0$ and a dielectric loss tangent $\text{tg}\,\sigma$ at different frequencies. The Fig. 4 shows the temperature dependences of the relative permittivity $\varepsilon(T)$ (*a*) and the dielectric loss tangent (*b*) for the ferroelectric compound $Bi_3Ti_{1.5}W_{0.5}O_9$ within the frequency range from 100 kHz to 1 MHz.

The maximum permittivity corresponding to the ferroelectric-to-paraelectric phase transition (T_C) is distinct at $T_C = 760°C$ (at the frequencies from 100 kHz to 1 MHz), the paper by Shi Luo et al. [21] specifies the Curie temperature $T_C = 730°C$. In our case, $T_C = 723°C$ corresponds to the maximum dielectric loss tangent before the phase transition. The peak relative permittivity $\varepsilon/\varepsilon_0$ approximately in 14 times exceeds the relative permittivity $\varepsilon/\varepsilon_0$ at the room temperature. The dielectric losses are very small, especially at the temperature below 300°C. With increase in the temperature, the dielectric losses increase to the temperature of 723°C and have a distinct maximum at all the measurement frequencies, and sharply decrease thereafter down to 754°C. Usually, the minimum dielectric losses are in advance of the peak permittivity by 5°C. With

further increase in the temperature, the dielectric losses sharply increase.

The activation energy E_a is determined from the Arrhenius equation:

$$\sigma = (A/T)\exp[-E_a/(kT)], \qquad (3)$$

where σ — electric conductivity, k — Boltzmann constant, A — the constant, E_a — the activation energy. The typical dependence $\ln\sigma$ (σ-conductivity) on $1/T$ (at the frequency of 100 kHz), which has been used to determine the activation energy E_a, is shown in the Fig. 5 for the AP $Bi_3Ti_{1.5}W_{0.5}O_9$. The compound $Bi_3Ti_{1.5}W_{0.5}O_9$ has two temperature ranges, in which the activation energy E_a significantly differs in the value. Within the lower temperatures, the electric conductivity is predominantly determined by impurity flaws with very low activation energies in order of several hundredths of the electron-volt.
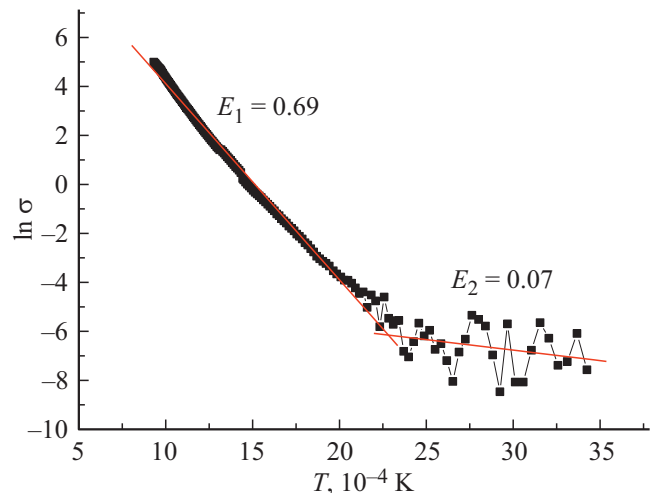

Figure 5. Dependence $\ln\sigma$ on $1/T$ for the sample $Bi_3Ti_{1.5}W_{0.5}O_9$.

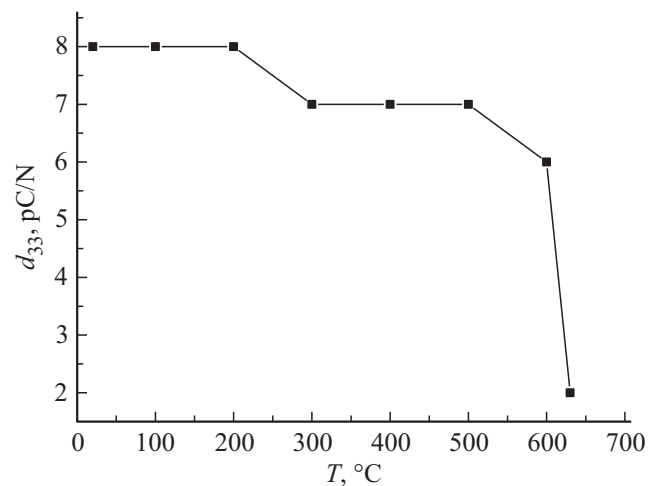**Figure 6.** Temperature dependence of the piezoelectric constant (d_{33}) $Bi_3Ti_{1.5}W_{0.5}O_9$

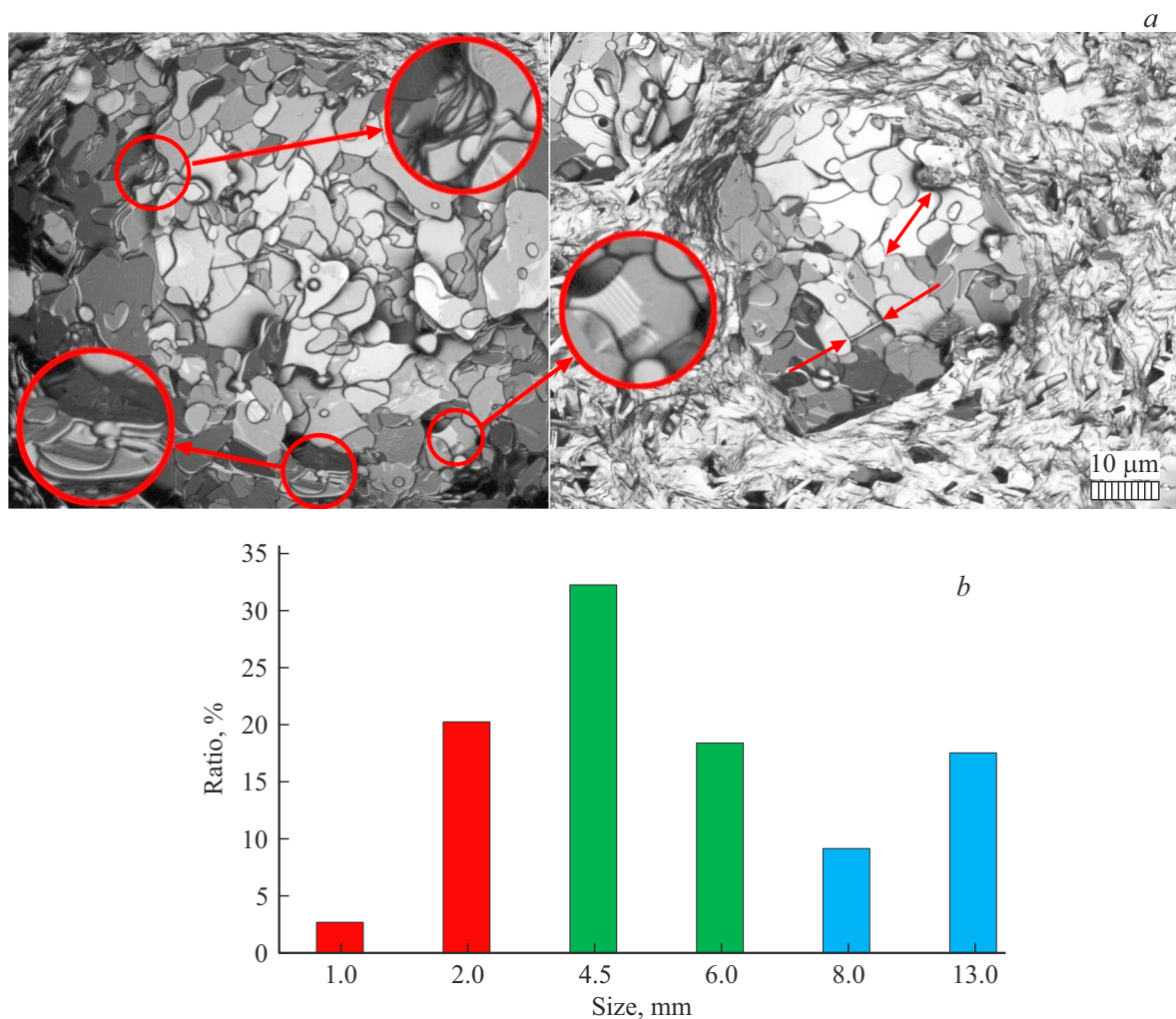**Figure 7.** SEM-images of the surfaces of transverse cleaved end face Bi$_3$Ti$_{1.5}$W$_{0.5}$O$_9$ (*a*) and grain size distribution (*b*).

For the compounds Bi$_3$Ti$_{1.5}$W$_{0.5}$O$_9$ we observe an area with prominent impurity conductivity within the temperature range from 20 to 450°C. Within the higher temperatures, the intrinsic conductivity prevails.

The Fig. 6 shows the dependence of the piezomodule (d_{33}) Bi$_3$Ti$_{1.5}$W$_{0.5}$O$_9$ on the temperature. The ceramic Bi$_3$Ti$_{1.5}$W$_{0.5}$O$_9$ exhibits good stability after thermal impact up to the temperature 550°C. The Table 2 gives a piezomodule value d_{33} for Bi$_3$Ti$_{1.5}$W$_{0.5}$O$_9$.

The Fig. 7, *a* shows SEM-images of the ceramic Bi$_3$Ti$_{1.5}$W$_{0.5}$O$_9$, baked at 1100 °C. It can be clear that the grains have a lamellar morphology, which typically characterizes the polycrystalline ceramic of the AP family. Such an anisotropic type is attributed to the fact that a grain growth rate in a plane $a-b$ is significantly higher than in the direction of the axis c of the crystal Bi$_3$Ti$_{1.5}$W$_{0.5}$O$_9$ due to the presence of hard layers (Bi$_2$O$_2$)$^{2+}$. The plane $a-b$ is parallel to a plane of the lamellar grains, while the axis c is parallel to an axis direction of the lamellar grains. The SEM-images of the ceramic Bi$_3$Ti$_{1.5}$W$_{0.5}$O$_9$ have the mixed lamellar grains of different orientation put up

together. A nature of crystallite arrangement has an evident stack of thin (0.5 μm) lamellar grains (Fig. 7, *a*, marked-up areas), which is also typical for the ceramic of the AP family. The sizes were estimated by taking into account all visible grains independent of their mutual arrangement. In doing so, a line of the biggest length was selected (Fig. 7, *a*, arrows).

The Fig. 7, *b* shows a histogram of the grain size distribution in percent to a total number of the grains on the surface of cleaved end face. It is clear that the main portion of the grains (about 70%) has the size of 2−6 μm, which confirms uniformity of their distribution. Together with a high density and low porosity of the ceramic and with no glass phase, it allows concluding that the selected baking conditions (1100°C) are optimal.

4. Conclusion

The solid-state method was used to synthesize the lamellar perovskite-like bismuth oxide Bi$_3$Ti$_{1.5}$W$_{0.5}$O$_9$ of the AP family. The X-ray diffraction study carried out in

the present paper has demonstrated that all the compound produced was a single-phase one with the rhombic crystal lattice ($A2_1am$, No 36).

The paper has determined the temperature T_C of the ferroelectric-to-paraelectric phase transition $T_C = 760°C$ and the optimal baking temperature $T = 1100°C$, and investigated a micro-structure of the surface of the cleaved end face of the ceramic $Bi_3Ti_{1.5}W_{0.5}O_9$ and measured the piezomodule $d_{33} = 8\,pC/N$. It is established that the lamellar perovskite-like bismuth oxide $Bi_3Ti_{1.5}W_{0.5}O_9$ of the AP family keeps its piezoproperties up to the temperature of $T = 550°C$.

Thus, the lamellar oxide of bismuth perovskite $Bi_3Ti_{1.5}W_{0.5}O_9$ of the AP family can be a base for creating new high-temperature lead-free piezoelectric & ferroelectric materials.

Acknowledgments

Conflict of interest

The authors declare that they have no conflict of interest.

References

[1] B. Aurivillius. Arkiv. Kemi. **54**, 463 (1949).
[2] B. Aurivillius. Arkiv. Kemi. **58**, 499 (1949).
[3] B. Aurivillius. Arkiv. Kemi. **37**, 512 (1950).
[4] G.A. Smolensky, V.A. Isupov, A.I. Agranovskaya. Physics of the Solid State **1**, 169 (1959).
[5] I.G. Ismailzade. Izv. AN SSSR **24**, 1198 (1960) (in Russian).
[6] B. Aurivillius. Phys. Rev. **12**, 6893 (1962).
[7] E.C. Subbarao. Am. Ceram. Soc. **45**, 166 (1962).
[8] E.C. Subbarao. Chem. Phys. **34**, 695 (1961).
[9] E.C. Subbarao. Phys. Rev. **122**, 804 (1961).
[10] E.C. Subbarao. Phys. Chem. Solids **23**, 665 (1962).
[11] S.V. Zubkov, V.G. Vlasenko. Physics of the Solid State **59**, 2325 (2017).
[12] S.V. Zubkov, S.I. Shevtsova. Adv. Mater. **6**, 173 (2020).
[13] T. Kikuchi. J. Less-Common Met. **48**, 319 (1976).
[14] Neil C. Hyatt, Ian M. Reaney, S. Kevin Knight. Phys. Rev. B **71**, 024119 (2005).
[15] W. Kraus, G. Nolze. PowderCell for Windows. Version 2.3. Federal Institute for Materials Research and Testing, Berlin, (1999).
[16] V.A. Isupov. Journal of Inorganic Chemistry **39**, *5*, 731 (1994).
[17] V.A. Isupov. Ferroelectrics **189**, 211 (1996).
[18] V.A. Isupov. Neorgan. materialy **421**, 353 (2006) (in Russian).
[19] V.M. Goldschmidt. Geochemische Verteilungsgesetze der Elemente. Norske, Oslo (1927).
[20] R.D. Shannon. Acta Crystallogr. A **32**, 75 (1976).
[21] Shi Luo, Y. Noguchi, M. Miyayama, T. Kubo. Mater. Res. Bull. **36**, 531 (2001).